Journal of
Ship&Ocean
Technology
© MARCH 2000

SOTECH Vol. 4, No. 1, pp. 1~10, 2000

Numerical Prediction of Open Water Performance of Flapped Rudders

S.-W. Pyo[1] and J.-C. Suh[1]

[1] Department of Naval Architecture and Ocean Engineering, Seoul National University, San 56-1, Shinrim-dong, Kwanak-ku, Seoul, 151-742, KOREA; E-mail: pyo@cavity.snu.ac.kr

Abstract

A low-order potential based boundary element method is applied for the prediction of the performance of flapped rudders as well as all-movable rudders in steady inflow. In order to obtain a reasonable solution at large angles of attack, the location of the trailing wake sheet is determined by aligning freely with the local flow. The effect of the wake sheet roll-up is also included with use of a high order panel method. The flow in the gap of a flapped rudder is modeled as Couette flow and its effect is introduced into the kinematic boundary conditions for flux at both the inlet and the outlet of the gap. In order to validate the present method, the method is applied for a series of rudders and the computational results on forces and moments are compared with experimental data. The effect of the gap size on the forces and moments is also presented.

Keywords: rudder, flap, surface panel method, roll-up

1 Introduction

In most marine applications, lifting devices have been used to control the motion of bodies. A rudder has been used to control the horizontal motion of a ship and a diving plane to control the vertical motion of a submarine. The forces and moments generated from the rudder determine the maneuvering characteristics of the ship. Therefore, it is essential in the design and assessment of the rudder to accurately predict and thus control its hydrodynamic characteristics.

Surface panel methods have been developed and applied successfully for the analysis of all-movable rudders(Gong et al 1992). In their method, however, the geometry of the trailing wake sheet is frozen as a prescribed surface and the resulting forces and moments of the rudders at large angles of attack have been found to be inaccurate. Most of the numerical methods have focused on the problem of all-movable rudders. For a flapped rudder, surface panel methods have given poor predictions of the forces and moments, mainly due to the inappropriate modeling of the gap flow between the main components and the flap.

In the present work, in order to predict accurately the effect of the wake sheet on the rudder, the location of the trailing wake sheet is determined from the *force-free* wake condition and the vortex sheet roll-up is included via a high order panel method(Pyo and Kinnas 1997). The flow in the gap of a flapped rudder is modeled as Couette flow(Kang 1993) for a channel and its effect is included in the application of the kinematic boundary condition on the inlet and the outlet panels

of the channel. The present method is first applied to the all-movable rudder and is extended for a series of flapped rudders. For its validation, the numerical results from the present method are compared with existing experimental data.

2 Numerical formulation

The fundamentals of the surface panel method have been described by many researches(Lee 1987, Hoshino 1989, Pyo 1995). The method is based on the classical Green's third identity for a perturbation potential ϕ.

$$2\pi\phi = \int_{S_B} \left[\phi\frac{\partial G}{\partial n} - G\frac{\partial \phi}{\partial n}\right] dS + \int_{S_W} \Delta\phi\frac{\partial \phi}{\partial n} dS \tag{1}$$

where S_B is the rudder surface and S_W its trailing wake surface.

In the present method, the rudder and its wake surface are discretized with hyperboloidal panels and constant strength dipoles and sources are distributed on the panels. The root section of the rudder is assumed to be attached to the hull so that the there is no cross flow over the root. Thus, the effect of the presence of the hull is included by an image method. The Kutta condition(Suh et al 1992), which requires the stagnation point at either the upper or the lower trailing edge as well as the pressure equality along the trailing edge of the rudder, is enforced numerically.

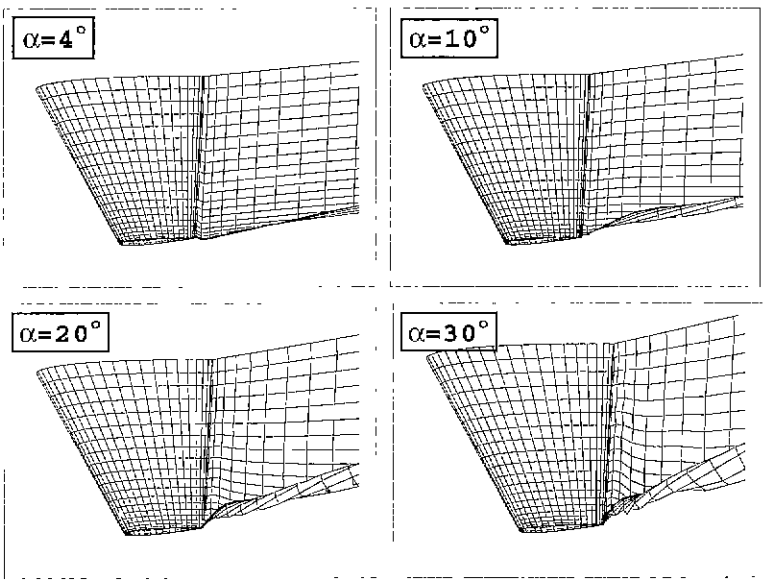

Figure 1: The trailing wake geometries of an all-movable rudder for four different angles of attack.

2.1 Trailing wake model

The geometry of the trailing wake sheet can be determined from the condition that each element of the trailing vorticity must be aligned with the local flow. In the surface panel method, it has

been suggested(Pyo 1995) that the use of a high-order panel method is more accurate than the low-order panel method to compute the local velocities on the trailing wake sheet, since it precludes the appearance of instabilities in the vortex sheet due to the spurious numerical effects introduced by a too crude representation. Since the local flow depends on the wake geometry in a nonlinear way, an iterative method should be applied.

In this work, the trailing wake sheet is modeled by piecewise dipole distributions with a bi-quadratic strength. Then the wake sheet is aligned with the local flow. This method has been extensively described by Pyo(1995). The resulting trailing wake geometries for four different angles of attack are shown in Figure 1.

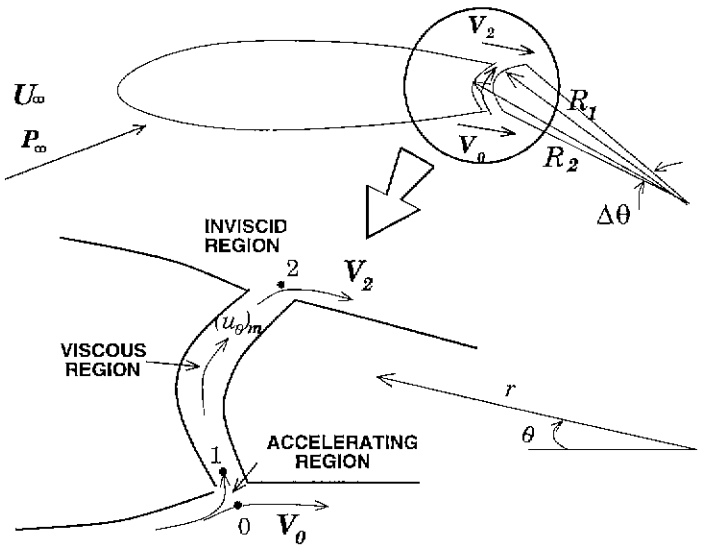

Figure 2: Two dimensional sketch of a flapped rudder with a gap.

2.2 Gap flow model

Consider the flow inside the gap between the forward and the after portion of the flapped rudder as shown in Figure 2. Since the gap connects the high-pressure region on the lower surface of the rudder to the relatively low-pressure region on the upper surface, the fluid enters into the gap at point 0, accelerates between point 0 and point 1, continues with a constant velocity $(u_\theta)_m$ and finally comes out of the gap at point 2 as shown in Figure 2. Thus, the pressure difference across the channel can be written as follows:

$$\begin{aligned}
\Delta p &= p_2 - p_0 = -\frac{1}{2}\rho\left(|\boldsymbol{V}_2|^2 - |\boldsymbol{V}_0|^2\right) = (p_2 - p_1) + (p_1 - p_0) \\
& p_2 - p_1 = \left(\frac{\partial p}{\partial \theta}\right)\Delta\theta \\
& p_1 - p_0 = -\frac{1}{2}\rho\left((u_\theta)_m^2 - |\boldsymbol{V}_0|^2\right)
\end{aligned} \tag{2}$$

where $\Delta\theta$ is the angular extent in radian between point 1 and point 2.

The gap flow between 1 and 2 can be considered as the flow maintained between two fixed concentric cylinders (R_2, R_1 are the radius of the outer and the inner cylinders, respectively). The solution for this problem in polar coordinates(r, θ) is straightforward and the leading term of the solution for the small gap is given by Kang(1993) as follows:

$$\begin{aligned} u_\theta(r) &\approx -\frac{1}{2\mu R_0}\left(\frac{\partial p}{\partial \theta}\right)(r-R_1)(R_2-r) \\ & R_0 = \frac{R_1+R_2}{2} \\ & h = R_2 - R_1 \end{aligned} \tag{3}$$

where u_θ is a velocity component in θ-direction and p is the pressure in a channel.

Then, the average velocity in a channel can be written:

$$(u_\theta)_m = \frac{1}{R_2-R_1}\int_{R_1}^{R_2} u_\theta(r)dr = -\frac{h^2}{12\mu R_0}\left(\frac{\partial p}{\partial \theta}\right) \tag{4}$$

By substituting (4) into (2), the equation (2) can be rewritten as follows:

$$\begin{aligned} & c_1\left(\frac{\partial \bar{p}}{\partial \theta}\right)^2 + c_2\left(\frac{\partial \bar{p}}{\partial \theta}\right) + c_3 = 0, \qquad Re = \frac{|\boldsymbol{U}_\infty|\, h}{\nu} \\ & c_1 = \frac{1}{576}Re^2\left(\frac{R_0}{h}\right)^2, \qquad c_2 = -\Delta\theta, \qquad c_3 = -\left(\frac{|\boldsymbol{V}_2|}{|\boldsymbol{U}_\infty|}\right)^2 \end{aligned} \tag{5}$$

where the non-dimensionalized pressure $\bar{p}$ is defined as $p/\frac{1}{2}\rho\,|\boldsymbol{U}_\infty|^2$.

From (5), $\partial p/\partial\theta$ can be found and the average velocity in the channel can be expressed by follows:

$$\frac{(u_\theta)_m}{|\boldsymbol{U}_\infty|} = \frac{12}{Re}\left(\frac{R_0}{h}\right)\left[-\Delta\theta + \sqrt{(\Delta\theta)^2 + \left\{\frac{Re}{12}\left(\frac{h}{R_0}\right)\left(\frac{|\boldsymbol{V}_2|}{|\boldsymbol{U}_\infty|}\right)\right\}^2}\,\right] \tag{6}$$

Notice that the average velocity in (6) is not equal to zero for the case of zero camber and zero angle of attack. This is because of the assumption that the velocity changes smoothly from the position 1 to he position 2. For the above case, the velocity at the position 1 is equal to zero but the velocity at the position 2 is not equal to zero.

The gap effect may be modeled via a kinematic boundary condition satisfied on the inlet and the outlet panel of the channel as follows:

$$\frac{\partial \phi}{\partial n} = -\boldsymbol{U}_\infty \cdot \vec{n} \pm (u_\theta)_m, \qquad \text{on the outlet/inlet panel} \tag{7}$$

2.3 Numerical Procedure

In order to include the effect of the gap and the aligned roll-up wake sheet, the following method is implemented.

(a) Solve (1) with a specified geometry of the trailing wake sheet, which is aligned with the inflow as an initial guess.

(b) Compute the velocity V_2 at the outlet panel of the channel and $(u_\theta)_m$ from (6).

(c) Solve (1) with a new kinematic boundary condition (7).

(d) Repeat step (b) and step (c) until the $(u_\theta)_m$ converges.

(e) Compute the induced velocities at the control points of the panels in the wake.

(f) Construct new wake geometry and solve (1) with the updated wake geometry.

(g) Repeat steps (e) to (f) until the geometry of the wake sheet is converged.

When the maximum relative difference δ_{max} is set to 0.01, for the converged solution, it usually takes three iterations for the average normal velocity in the gap and two iterations for the wake sheet roll-up.

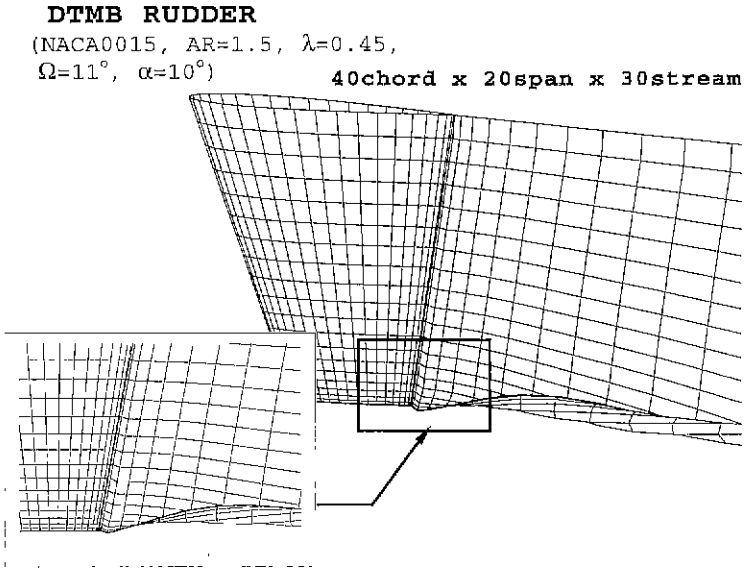

Figure 3: Panel arrangement for the DTMB rudder. There are 40 chordwise and 20 spanwise panels on the rudder surface

3 Numerical results

3.1 All-movable rudder

The method is first applied to an all-movable rudder in uniform inflow. For all-movable rudders, DTMB developed empirical formulae for forces and moments based on their extensive experimental data(Whicker and Fehlner 1958). The calculation is done for a DTMB rudder. The rudder has an NACA0015 section with geometric aspect ratio $AR = 1.5$. The taper ratio is 0.45 and the sweep angle is 11^o. In the present calculations, the panels are distributed using cosine spacing in the chordwise direction and half-cosine spacing in the spanwise direction. The panel arrangement for the rudder is shown in Figure 3. Figures 4 and 5 show C_L, C_D and C_M over a range of angle of attack α.

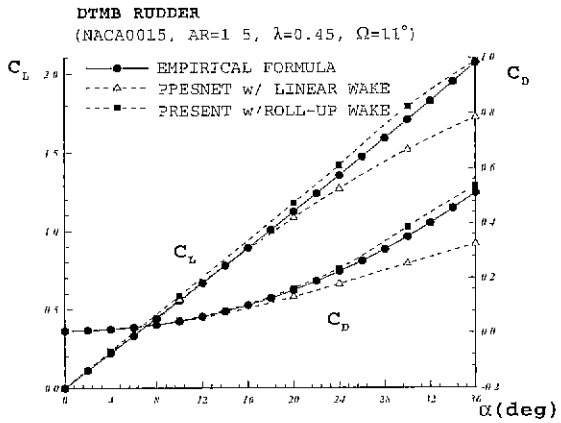

Figure 4: Comparison of measured and calculated C_L, C_D for an all-movable rudder with an NACA0015 section; taper ratio=0.45, aspect ratio=1.5.

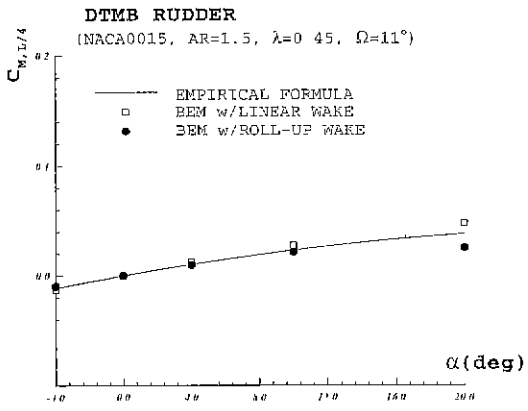

Figure 5: Comparison of measured and calculated C_M for an all-movable rudder with an NACA0015 section; taper ratio=0.45, aspect ratio=1.5.

It is noticed from the figures that C_L and C_D calculated with the aligned wake geometry have higher values than those with the straight wake geometry and show good agreement to the experimental data for large angles of attack ($\alpha > 20^o$). When the angle of attack is less than 20^o, both numerical results show very good agreement to the experimental data.

3.2 Flapped rudder

Kerwin et al(1972) tested a series of flapped rudders in a water tunnel while varying the amount of flap area and flap angle. The experiments were run at a Reynolds number of about 1.2×10^6 and the minimum gap was 0.2% of the span. For the present calculation, No.2 rudder in Kerwin et al(1972) is chosen. The rudder has 30% flap and an NACA66 thickness distribution with geometric aspect ratio $AR = 1.4$. The taper ratio is 0.6 and the sweep angle is 11^o. Other specifications are given in Kerwin et al(1972)

Panel arrangements for the calculation of the flapped rudder are shown in Figure 6 for the case of four different angles of attack. It is noticed that the smooth roll-up is obtained in all cases.

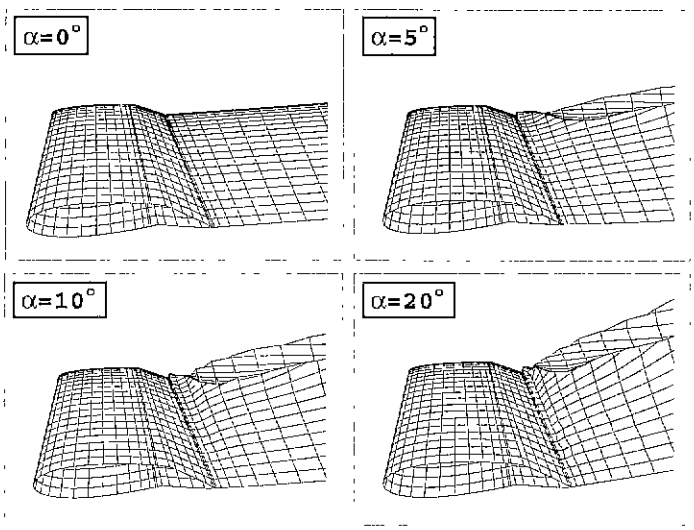

Figure 6: The trailing wake geometries of a flapped rudder for four different angles of attack.

Figures 7, 9 and 11 show that C_L and C_D characteristics of the flapped rudder with $0^o, 10^o, 20^o$ flap angles, respectively. The resulting forces obtained with the gap flow model show better agreement to the experimental data than those ignoring the gap flow effect. As the flap angle increases, the difference from the experimental data becomes larger but it is still acceptable. In the viewpoint that there may be stall when α is greater than 15^o, the numerical results with the present gap flow model are very encouraging. Figures 8, 10 and 12 show C_M with $0^o, 10^o, 20^o$ flap angles, respectively. It is noticed that C_M shows the same trend as that of C_L, C_D but the big difference from the experiment data occurs at zero angle of attack.

Figures 13 and 14 show that C_L, C_D and C_M characteristics of the rudder with 10^o flap for the gap clearance of $0\%, 0.01\%, 0.2\%$ and 1% to the rudder span. It is found that the gap size is not the important factor for the forces and moments calculation.

4 Conclusions

A surface panel method for the analysis of a series of rudders in uniform flow is presented. The aligned wake sheet model containing the roll-up effect improves the predicted forces and moments for large angles of attack. A gap flow model is used in order to improve the numerical accuracy for a flapped rudder. In order to validate the present method, the computed force and moment coefficients are compared to those from existing experimental data. The resulting forces and moments are found to be closer to the experimental values. Finally, it is concluded that the proposed method can be used to predict rudder forces and moments reasonably well unless stall occurs.

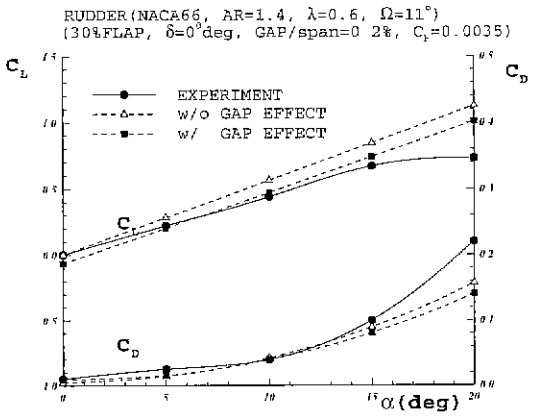

Figure 7: Comparison of measured and calculated C_L, C_D for a flapped rudder with an NACA66 section; taper ratio=0.6, aspect ratio=1.4, flap angle=0^o.

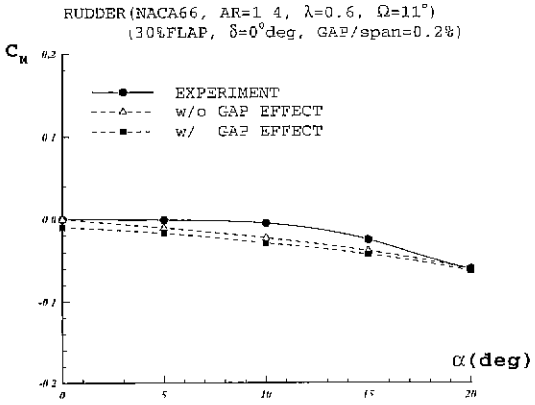

Figure 8: Comparison of measured and calculated C_M for a flapped rudder with an NACA66 section; taper ratio=0.6, aspect ratio=1.4, flap angle=0^o.

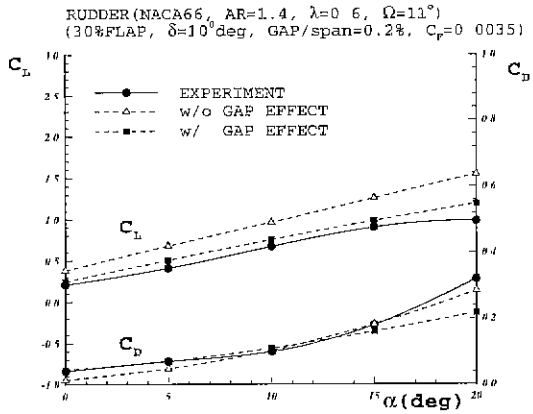

Figure 9: Comparison of measured and calculated C_L, C_D for a flapped rudder with an NACA66 section; taper ratio=0.6, aspect ratio=1.4, flap angle=10^o.

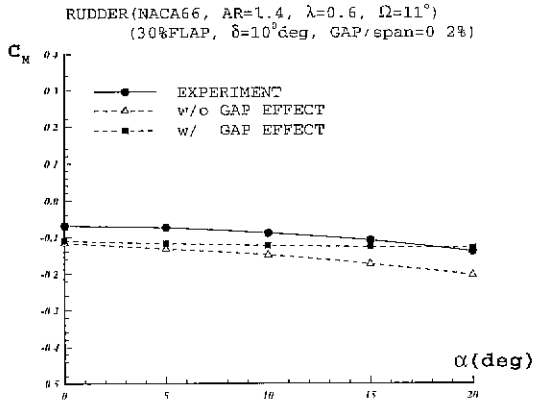

Figure 10: Comparison of measured and calculated C_M for a flapped rudder with an NACA66 section; taper ratio=0.6, aspect ratio=1.4, flap angle=10^o.

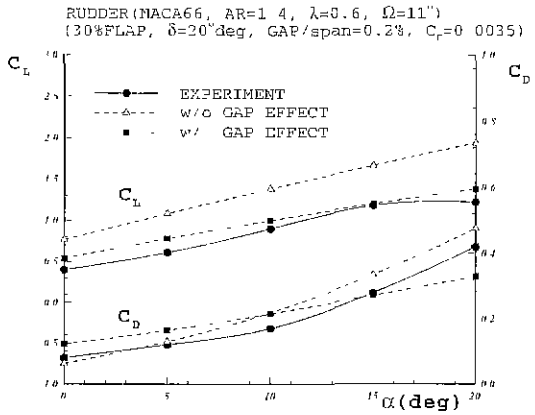

Figure 11: Comparison of measured and calculated C_L, C_D for a flapped rudder with an NACA66 section; taper ratio=0.6, aspect ratio=1.4, flap angle=20^o.

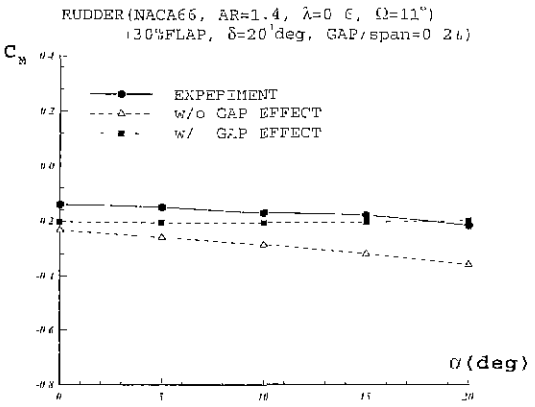

Figure 12: Comparison of measured and calculated C_M for a flapped rudder with an NACA66 section; taper ratio=0.6, aspect ratio=1.4, flap angle=20^o.

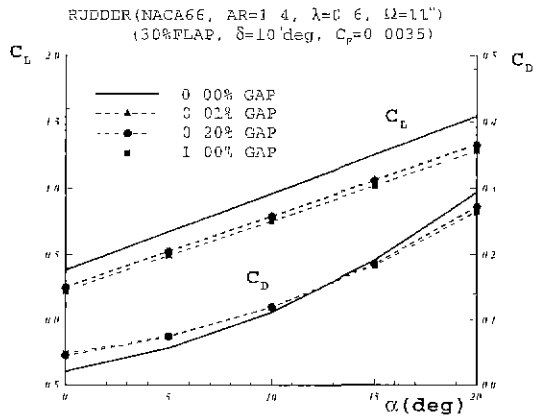

Figure 13: Comparison of measured and calculated C_L, C_D for a flapped rudder with an NACA66 section; taper ratio=0.6, aspect ratio=1.4, flap angle=20^o.

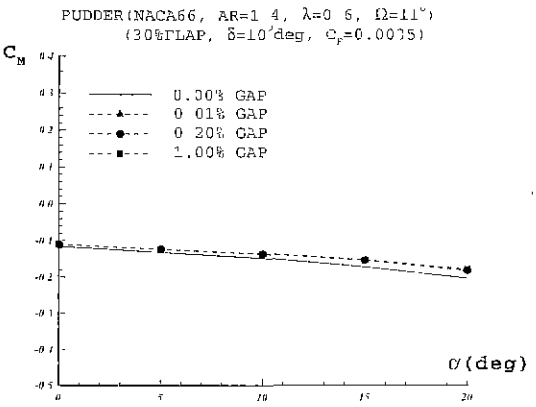

Figure 14: Comparison of measured and calculated C_M for a all-movable rudder with an NACA66 section; taper ratio=0.6, aspect ratio=1.4, flap angle=20^o.

References

GONG, I.Y., KANG, C.G. AND LEE, C.M. 1992 Theoretical analysis of open water characteristics of a rudder. J. of the Society of Naval Architects of Korea, **29**, **1**, pp. 29-42

HOSHINO, T. 1989 Hydrodynamic analysis of propellers in steady flow using a surface panel method. Proceedings, Spring Meeting of Society of Naval Architects of Japan

KANG, C.G. 1993 *Effect of a gap of a 2-D flap rudder on the lift.* J. of the Society of Naval Architects of Korea, **30**, **4**, pp. 31-38

KERWIN, J.E., MENDEL, P. AND LEWIS, S.D. 1972 An experimental study of a series of flapped rudders. J. of Ship Research, **16**, **4**, pp. 221-239

LEE, J.T. 1987 A potential based panel method for the analysis of marine propellers in steady flow. PhD Thesis, Department of Ocean Engineering, MIT

PYO, S. 1995 Numerical modeling of propeller tip flows with wake sheet roll-up in three dimensions. PhD Thesis, Department of Ocean Engineering, MIT

PYO, S. AND KINNAS, S.A. 1997 Propeller wake sheet roll-up modeling in three-dimensions. J. of Ship Research, **41**, **2**, pp. 81-92

SUH, J.C., LEE, J.T. AND SUH, S.B. 1992 A bilinear source and doublet distribution over a planar panel and its applications to surface panel methods. Proceedings, Nineteenth Symposium on Naval Hydrodynamics

WHICKER, L.F. AND FEHLNER, L.F. 1958 Free stream characteristics of a family of low aspect ratio, all-movable control surfaces for application to ship design. DTMB Report, No. 933